

Durham Research Online

Deposited in DRO:

29 May 2018

Version of attached file:

Accepted Version

Peer-review status of attached file:

Peer-reviewed

Citation for published item:

Mikołajczyk, Łukasz and Milek, Karen (2016) 'Geostatistical approach to spatial, multi-elemental dataset from an archaeological site in Vatnsfjörur, Iceland.', *Journal of archaeological science : reports.*, 9 . pp. 577-585.

Further information on publisher's website:

<https://doi.org/10.1016/j.jasrep.2016.08.036>

Publisher's copyright statement:

© 2016 This manuscript version is made available under the CC-BY-NC-ND 4.0 license
<http://creativecommons.org/licenses/by-nc-nd/4.0/>

Additional information:

Use policy

The full-text may be used and/or reproduced, and given to third parties in any format or medium, without prior permission or charge, for personal research or study, educational, or not-for-profit purposes provided that:

- a full bibliographic reference is made to the original source
- a [link](#) is made to the metadata record in DRO
- the full-text is not changed in any way

The full-text must not be sold in any format or medium without the formal permission of the copyright holders.

Please consult the [full DRO policy](#) for further details.

Geostatistical approach to spatial, multi-elemental dataset from an archaeological site in Vatnsfjörður, Iceland

Łukasz Mikołajczyk and Karen Milek, University of Aberdeen.

1. Introduction

Understanding the spatial patterning of human activity is of crucial importance to the interpretation of any archaeological site. Not every site has a well-defined stratigraphy, or a material record, that can be used to grant insight into the nature of the activities that were undertaken, and how these were distributed. In such cases, geochemistry can provide a cheap and effective solution for characterising the use of archaeological space. The core principle behind archaeological geochemistry is that human activity causes chemical distortion (enrichment or depletion) to the local substrate (Oonk et al. 2009, Middleton et al. 2010 with references). This chemical signal can be used to 'fingerprint' the types of activities that were taking place. There are, however, limitations to the method linked to difficulties in differentiating the origin of the chemical signal (Oonk et al. 2009). For example, problems arise when attempting to identify multiple deposition episodes, through the possible influence of diagenetic processes in altering the chemical signal (Middleton et al. 2010), and as a consequence of the statistical methods used to process multivariate datasets (Entwistle et al. 2007; Dore and Lopez Varela 2010). In this paper we highlight this problem and tackle it through the application of the methodological framework proposed by Dore and Lopez Varela (2010) with some modifications. Rather than using only a limited suite of soil-chemical measurements (i.e. phosphates, carbonates, pH, protein residues, and fatty acids), we adopt an approach in which a multi-elemental dataset is produced and analysed. In doing so we highlight the statistical procedures that we consider to be the most crucial for an informed interpretation of human activity at an archaeological site, using a farm in Iceland as our reference case. At this location, the interplay between human pressure and natural processes (e.g. relative sea level change) was considered important in influencing the pattern and character of activity, and therefore a method for establishing a wide range of elements was used (X-ray fluorescence). In such a situation, not only is the anthropogenic signal able to be studied, but also the natural processes affecting the site can be taken into consideration (Linderholm and Lundberg 1994).

Geochemical studies of coastal archaeological sites are not unusual (see Knudson 2004; Ilves and Darmark 2011 with references; Misarti et al. 2011). There are several studies of this type in Iceland; most have used phosphate (P) analysis (Bolender, 2003; 2006; Simpson et al., 2002; Mikołajczyk et al. 2015), and there is one multi-elemental study (Milek and Roberts 2013). This paper builds on previous research in this field through the application of

38 archaeological geochemistry to the iron- and allophone-rich andosols that are specific to
39 Iceland (Arnalds et al., 1995; Arnalds, 2004).

40

41 2. Study area

42 The farm of Vatnsfjörður is located in the Vatnsfjörður fjord, northwest Iceland, and has
43 been continuously occupied from the 10th century AD to the present day. Written sources
44 mention Vatnsfjörður as one of the original *landnám* farms that in the 12th and 13th
45 centuries served as a Chieftain's seat. It was also the location of a church reputed to be the
46 second wealthiest on the island. The site kept its privileged position until the end of 16th
47 century. The site consists of three components (Fig. 1, left): the Viking-age settlement area,
48 the Medieval to Early-Modern farm mound, and an extensive coastal zone (Milek 2011: 17-
49 22). The coastline in the Vatnsfjörður area is not stable. Glacio-isostatic crustal movement
50 and glacio-eustatic sea-level rise are responsible for relative sea-level (RSL) changes in the
51 area. RSL was at least 1 m greater than at present during the mid-Holocene, subsequently
52 gradually falling to the present-day level (Norðdahl and Pétursson 2005; Lloyd and Dickens
53 2011; Mikolajczyk et al. 2015).



54
55 Fig. 1. The archaeological site of Vatnsfjörður: Left, aerial photography of the site. Visible are the Viking age,
56 Medieval and Early-Modern settlements plus the coastal zone, studied excerpt and control sampling area.
57 Right, enlarged studied section of the coastal zone. Visible, in red, are the extents of v-shaped (left) and u-
58 shaped (right) structures' collapsed material; in blue, structural walls; in black, the location of sampling points.

59 The archaeological coastal zone at Vatnsfjörður stretches c. 1500 m along the shoreline and
60 consists of three pronounced subzones, all of which still bear visible traces of intensive use

in the past (Fig. 1). All three were targeted with small scale archaeological investigations (Mikołajczyk and Gardela 2010: 48; Mooney et al. 2012: 49-50; Mooney 2013: 40-48, Mikołajczyk 2013) and phosphorous (P) transect mapping (Mikołajczyk et al. 2015). The most complex situation was encountered in Zone B where at least two, not necessarily chronologically-discrete phases of activity of unknown intensity merge in a relatively small area. Henceforth results were deemed insufficient to understand the character of human occupation in this area and for this reason extensive multi-elemental mapping of the area was employed, the results of which are presented in this paper. Zone B is located at the southernmost edge of Vatnsfjörður and is dominated by the ruin of a massive, 15 m long, U-shaped building (Fig. 1B) (Mikołajczyk and Gardela 2010: 48). It has been excavated (Mooney et al. 2012: 49-50, Mooney 2013: 40-48), but despite the detailed information on its construction method – the building is characterised by a very robust, 1.5 m thick, stone-lined, turf wall – its function remains unknown. It yielded neither datable material nor any other finds, and its internal floor layer is very thin and non-diagnostic (Mikołajczyk 2013). The shape of the building is similar to boathouse constructions. Results of the P mapping (Mikołajczyk et al. 2015) revealed an unusual orientation, parallel to the modern shoreline, facing the embayment at times when sea level was higher. The aforementioned research managed to date the activity area in front of this structure to the late 15th century on the basis of its elevation relative to sea level at this that time; this agrees with the general *ante quem* date for human activity in the zone that is stratigraphically below the tephra from eruption of Hekla dated to AD 1693. There are also three other ruins in the northern part of zone B, all of which are in a rather poor state of preservation (Fig. 1B). Two of them are c. 6 m long, V-shaped, overlapping boathouse-like structures and the third is a small, rectangular, stone-lined structure with walls abutting a natural bedrock outcrop. The activity area immediately east of the V-shaped structures was dated to late 12th century. The age of the rectangular structure is unknown. In the area to the west of the V-shaped structure, a slight depression in the terrain was noticed. A test trench placed there yielded some burnt seaweed fragments.

3. Methods

3.1. Sampling

316 soil samples were taken from 0.2x0.2 m shovel test pits placed according to a 1x1 m grid fixed on cardinal directions. Grid points were recorded with the use of a Trimble DGPS unit, with 1 cm accuracy. Special care was taken to sample soil strata recognised as corresponding to the archaeological structures. However, due to the thinness of the soil and the patchiness of the only chronological marker on the site (the H-1693 tephra layer), in some cases, samples had to be taken at an arbitrary depth of 0.05 m below the dense grass root mat (as that was the average depth of the H-1693 tephra when present). Additionally, a control group of 20 soil samples was taken in an opportunistic manner from two neighbouring areas without any visible archaeological features (Middleton and Price 1996).

100 3.2. Sample processing

101 336 samples, each weighing c. 20 g (dry), were oven dried, gently pulverized and
102 subsequently analyzed using an Olympus-Innov-X Delta Premium XRF scanner stocked with
103 Au anode tube. The device was operated in a 3 beam 'soil' calibration mode and in a
104 desktop setup allowing for convenient long exposure times. Prior to the main analysis,
105 reference material (soil samples with known elemental ratios) was tested multiple times in
106 order to select the exposure time that provided best repeatability. Samples were analyzed
107 for S, K, Ca, Ti, V, Mn, Fe, Cu, Zn, Br, Rb, Sr, Zr in the following set up: beam 1 - 40kV at 30s
108 exposure time; Beam 2 – 40kV at 30s exposure time; Beam 3 – 15kV at 60s exposure time.
109 All results are semi-quantitative.

110 4. Analysis

111 Due to the apparatus characteristics some P readings (c. 5%) yielded relatively high
112 detection errors. In order to account for this, problematic readings were corrected with a
113 use of values sub-sampled from the interpolation curve created on the base of the
114 remaining dataset. Readings for Ca, Mn, Fe and Cu yielded few outliers that in order to
115 maintain a more natural distribution of the data set were managed by winsorisation
116 (Chambers et al. 2000). Before computation, the data were standardized to avoid scaling
117 effects and to obtain average-centered distributions (Baxter 1995)

118 4.1 Spatial analysis

119 The spatial analysis was conducted using ArcGIS 10.2 (ESRI 2015) in a manner similar to that
120 followed by Dore and Lopez Varela (2010). The readings at sampling points for separate
121 elements were projected in a 2D space according to their x-y position on the site grid.
122 Subsequently, respective surfaces were interpolated by ordinary kriging. When necessary, in
123 order to account for potential directional influences, the second polynomial trend was
124 removed and interpolation weights were adjusted for anisotropy, the aim being to obtain a
125 model with the best cross-validation scores. Surfaces were subsequently turned into
126 elemental raster layers with floating point pixel type in 32 bit color depth with pixel size of
127 0.1 m. (Fig. 2). The rasters were subjected to principal component analysis (Pearson 1901,
128 Hotelling 1933). This procedure allows not only the 'noise' to be removed from the dataset,
129 but it also eliminates redundancies caused by highly correlated variables (Table 1). With the
130 use of the data fusion technique, this allows for efficient visual inspection of the spatial
131 structure of variance (Craig et al. 2006; Devereux et al. 2008; Kvamme 2006, 2007; Richards
132 and Jia 1999). The first three components that usually explain a gross part of variance were
133 plotted as red, green and blue channels of a composite raster, presenting a multi-color
134 representation of data spatial variability (Fig. 3.). Correlation coefficients of elemental and
135 component rasters were calculated indicating elemental loadings for particular components
136 (Fig. 4 and Table 2). Subsequently, elemental rasters were subjected to unsupervised
137 classification using an iterative self-organizing (ISO) clustering algorithm and a Maximum

Likelihood Classification tool. Various numbers of determined classes were considered with the goal being to obtain a classification that is visually the most concordant with the principal component raster, and most meaningful with regards to the site's spatial variability. Finally, a seven class output was chosen (Fig. 5) and all sampling points were grouped according to the class affiliation (Fig. 6).

Elements		Correlation coefficient
Ti	V	0.92
Ca	Sr	0.86
K	Zr	0.81
Zn	Sr	0.79
Ca	Zn	0.75
Ca	Br	-0.74
Ca	Mn	0.71

Table 1: List of the most highly correlated elements (correlation coefficient >0.7).

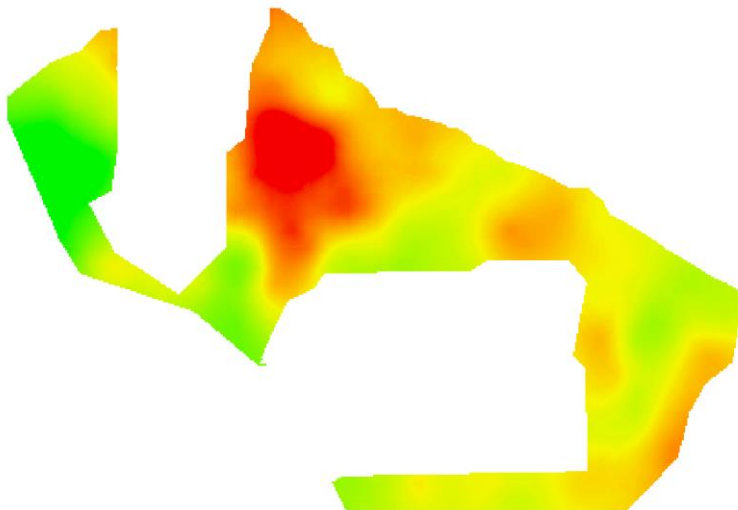
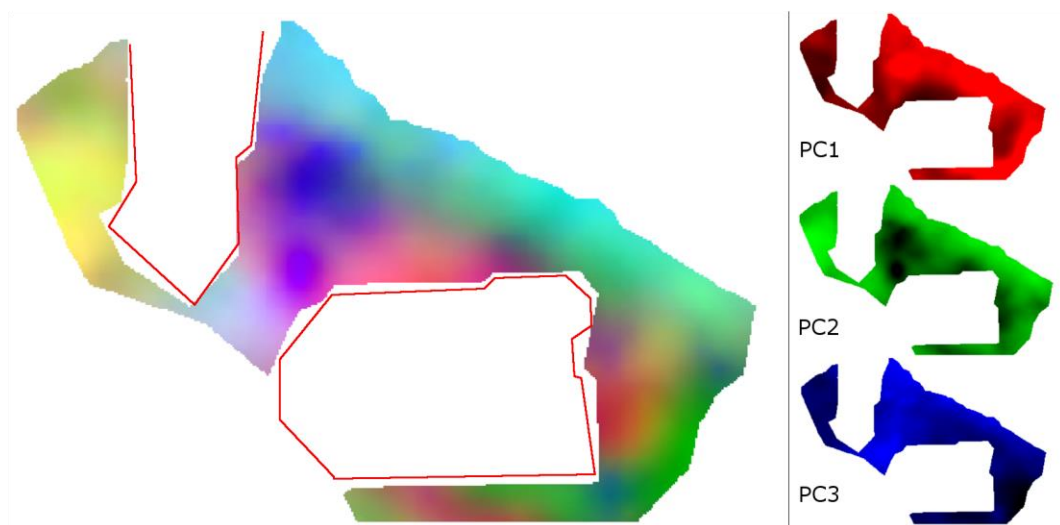


Fig. 2: An example of an interpolated elemental raster (for phosphorus) with values on the scale from low (green) to high (red).

4.2 Computational analysis

Further calculations were conducted on the raw data in using R software (R Core Team 2014). Class summary statistics were calculated and compared with the mean of on-site values. Deviations from the mean on two levels (>0.5 s.d. and >1.0 s.d.) were recorded (Table 3). Together with the PCA matrix (Fig. 4), these serve as a base for class interpretation.



4.2.1 PCA results

Fig. 3: Spatial projection of the Principal Component Analysis (PCA) results. Right: spatial distribution of variance for separate components depicted in red, green and blue; positive loadings - lighter, negative loadings- darker. Left: data fusion, tree components projected jointly with the outlines of buildings depicted in red.

Components	PC1	PC2	PC3
P	0.55	-0.61	0.34
S	-0.46	-0.78	0.16
K	0.45	0.16	0.78
Ca	0.37	0.54	-0.07
Ti	0.61	-0.38	0.32
V	0.84	-0.34	-0.20

Mn	0.84	-0.37	-0.06
Fe	0.33	-0.84	0.03
Cu	0.94	0.13	-0.03
Zn	0.62	0.16	0.53
Br	-0.83	0.11	0.36
Rb	-0.15	0.17	0.79
Sr	0.79	0.45	0.10
Zr	0.75	0.37	0.09
<hr/>			
% of variance	53.22	18.59	10.31
Accumulative % of variance	53.22	71.81	82.12

165 Table 2: Results of the Principal Component Analysis showing components' loadings and the % of variance
166 explained.

167 Three principal components, chosen for analysis according to Guttman-Kaiser criteria
168 (Guttman 1954; Kaiser 1960, 1970), accounted for 82.12 % of the total variance of the
169 geochemical record (Table 2).

170 The first principal component (PC1) accounts for 53.22 % of the explained variance with high
171 positive correlation coefficients for Sr, Zr, V, Mn, Cu (>0.75 $p=0.05$), moderate positive
172 correlation coefficients for P, Zn, and Ti (>0.55 $p=0.05$), and a high negative correlation
173 coefficient for Br (0.83 $p=0.05$).

174 The second principal component (PC2) accounts for 18.59% of the explained variance and is
175 dominated by redox sensitive elements (S and Fe) with high negative correlation coefficients
176 for (<-0.78 , $p=0.05$), a moderately negative correlation coefficient for P (-0.61 , $p=0.05$), and
177 moderately positive correlation coefficient for Ca (0.54, $p=0.05$).

178 The third principal component (PC3) accounts for 10.31 % of the explained variance and
179 reflects high positive correlation coefficients for K and Rb (>0.78 $p=0.05$), and a moderately
180 positive correlation coefficient for Zn (0.53 $p=0.05$).

181 4.2.2. PCA interpretation

182 *PC1*

183 The positively correlated elements for PC1 seem to represent, at least in part, the general,
184 local characteristics and the natural variability of elements across the site. This group
185 includes some elements indicative of marine environments such as Sr, V, P (Turekian 1964;
186 Blotcki et al. 1979; Franklin 2003; Schofield et al. 2010), the origin of which might be sea
187 spray or wave activity. Additionally, this component concentrates almost half of the

variance for P, which in the case an archaeological site could suggest a contribution to this component from human activity (Holiday and Gartner 2007). A concomitant strong negative correlation for Br, a universal marine organic matter indicator (Mayer et al. 1981; Ziegler et al. 2008), complicates the interpretation. It is quite possible that the P content is a terrestrial anthropogenic component reworked by the marine environment (e.g. wave activity) and the influx of Br was due to the sea spray vector (Shotyk et al. 2003), but such a discordance between two organic matter indicators is suspicious and might indicate that the original elemental ratios were heavily distorted by diagenesis. Positive contributions of Cu, Zr, and Zn can possibly be linked with atmospheric anthropogenic pollution (Küttner et al. 2014) as a consequence of metalworking, with pollutants presumably transported and deposited by tidal and wave activity. Spatially, the PC1 raster high positive readings are concentrated over the central spot between the two structures, in the coastal area and especially in the strip on the bank of the stream channel (Fig. 3). It seems that the positive readings are somewhat related to the presence and dynamics of water. Negative readings distinguish the area west to the V-shaped structure and area on the side of the U-shaped structure. These zones interpreted as showing very little marine influence.

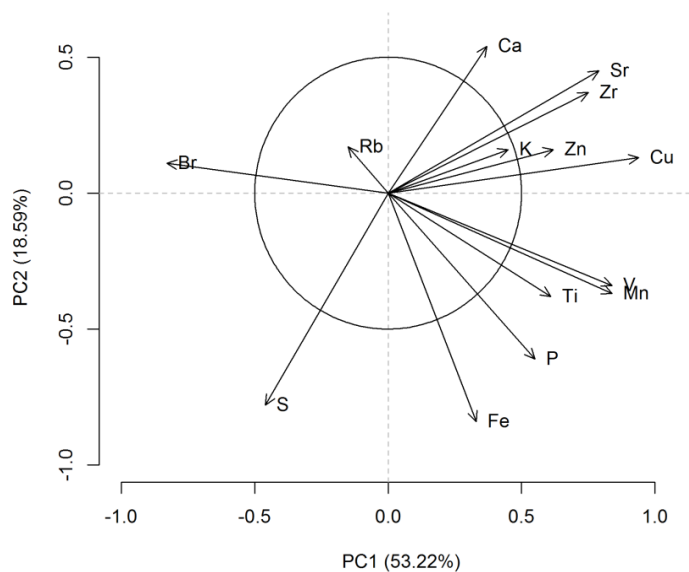


Fig. 4: Results of the Principal Component Analysis: the correlation matrix.

PC2

The second principal component seems to represent the biogenic contribution and is most likely to have captured any localized anthropogenic enrichment with high negative loadings from S and Fe sharing part of the P variance with PC1. This set of elements can be associated with habitation (Lutz 1951; Aston et al. 1998; Wilson 2009), the deposition of organic matter (Brady and Weil 1999, Milek and Roberts 2013; Supplement data table 3), and burning or ash deposition (Evans and Tylecote 1967; Willson et al. 2007; Milek and Roberts 2013;

Supplement data table 4). The spatial pattern of the negative readings is somewhat similar to PC1, being concentrated in a area between the structures, and also on the side and directly in front of the U-shaped building.

PC3

The third principal component demonstrates high positive loadings for lithogenic elements (K, Rb, Zn) and most likely captures the results of sedimentation on site (Shotyk 1988; 2003) and presumably some disturbance through anthropogenic activities. The spatial patterning distinguishes separate zones of high positive loading between the two structures balanced by opposite readings west of the V-shaped structure and on the bank of the stream.

Most of the elements discussed here are often present in tephra (Jagan 2010; Hayward 2011). There is a tephra layer – Hekla 1693 – present in patches in the Vatnsfjörður area and it is worth to keeping in mind that even though special care was taken to sample below it, there is a possibility that due to the disturbances in stratigraphical column some of the samples might have been contaminated with ash.

4.3 Cluster analysis

4.3.1 Clustering

The composite raster consisting of three component rasters bands representing red, green and blue channels illustrates the variability of the site's elemental composition based on the PCA results. Even though there are patterns emerging that clearly separate some areas from others (e.g. the west of the V-shaped structure is distinct from the area inbetween the two structures), the boundaries remain fuzzy. Thus, in order to efficiently divide the area of study into discrete zones, and to obtain elemental summary statistics, clustering on elemental rasters was performed (see Methodology section for details). Finally, a seven class division was chosen as the one best representing the zonation (Fig. 5). A dendrogram (Fig. 6) shows relative differences between the classes with notable affinity for classes 1, 2 and 3. Additionally, distribution of those three classes is not limited to a single location as it is characteristic for the remaining 4 classes; they are present in lcoations in the center of the sampled area. No other close grouping of classes is visible and subsequent the classes that have been distinguished are increasingly different. Additionally, they tend to describe discrete areas on the margins of sampled area.

4.3.2 Class chemical composition

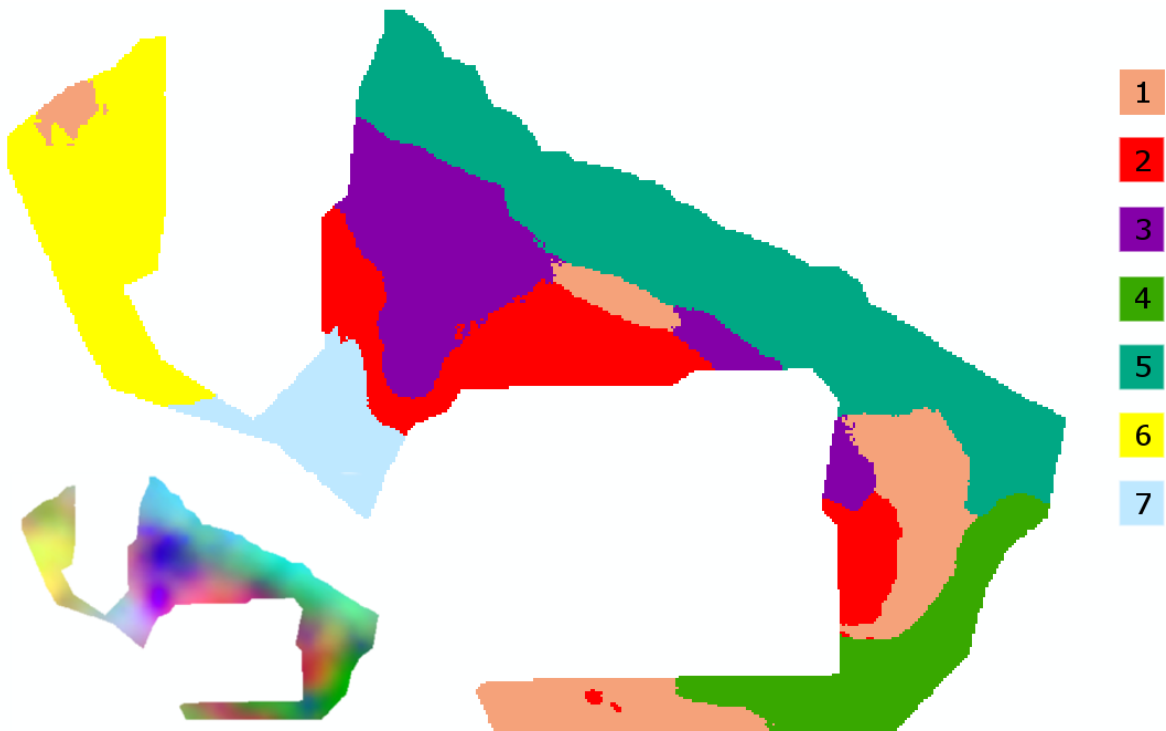


Fig. 5: Spatial distribution of the classes described in the text (the results of the Principal Component Analysis data fusion are also depicted for comparison in lower left corner of the diagram).

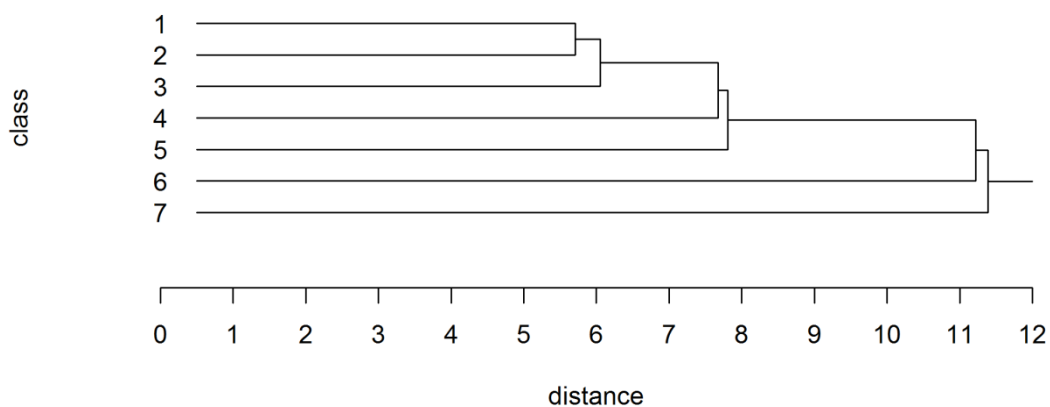


Fig. 6. Class dendrogram

Mean values of elemental readings for each class were compared with the site mean (Table 3) in order to understand the key differences between classes. Additionally, class mean values were compared with control sample means, although the first approach was favoured as a method for characterizing classes as certain doubts arose with regards to

control samples being sterile from anthropogenic impact. Enrichment and depletion were specified as moderate when they differed from the mean by more than 0.5 σ and less than 1.0 σ , and strong when they differed from the mean by more than 1.0 σ .

Full consideration was given to obtaining the most reliable control groups, but the elemental readings that were produced are rather unusual (see values for C1 and C2 in Table 3). As there is uncertainty with regards to control group sterility, the interpretation presented below is based on the class comparison versus the site mean. Control values are presented for inspection only.

263

vs. Site	P	S	K	Ca	Ti	V	Mn	Fe	Cu	Zn	Br	Rb	Sr	Zr
1	v	v	v	^	^	^	v	^	v	v	vv	v	v	^
2	v	^^	v	vv	v	v	v	^	v	vv	^^	v	vv	v
3	^^^	^^	^	^	^	^	^^	^^^	v	^	v	v	v	v
4	v	vv	v	^^	^^^	^^^	^	^	^	^^	vvv	vv	^^	^
5	^	vv	^	^^	^	^	^	v	^	^	v	^	^^	^
6	vv	v	vv	vv	vvv	vvv	vv	vvv	^	v	^^	v	v	vv
7	vv	v	^^	vvv	vv	vv	vv	vv	v	v	^^^	^^^	vvv	^^
C1	vv	v	v	v	^^	^^	v	vv	v	vv	^	^	^^	^
C2	v	^	vvv	^^^	^^^	^^^	^^	^	^^^	^^^	vv	vvv	^^^	v

264

Table 3: Class elemental means (rows 1-7 , with two control groups, C1 and C2) in relation to the overall site mean. Scale runs from from strongly depleted ('vvv' in dark green) to strongly enriched ('^^^' in dark red). Signature description: $\bar{x} - \sigma/2 \leq 'v' < \bar{x}$; $\bar{x} - \sigma < 'vv' < \bar{x} - \sigma/2$; $'vvv' \leq \bar{x} - \sigma$; $\bar{x} + \sigma/2 \geq '^' > \bar{x}$; $\bar{x} + \sigma > '^^' > \bar{x} + \sigma/2$; $'^^^' \geq \bar{x} + \sigma$.

The readings of P are to be treated with caution as there are reported cases of difficulties in obtaining phosphorous readings from Icelandic soils (Bolender, 2003: 42; 2006: 126; Simpson et al. 2002: 433; Mikolajczyk et al. 2015: 3). In this case, an indication that the P readings might in some way be biased is seen in the behaviour of P when measured against Br. Bromine is usually regarded as a reliable indicator of marine organic matter in a coastal environment (Mayer et al. 1981, Ziegler et al. 2008), and its behaviour should, to some degree, mimic that of P (another organic matter indicator; Olsen et al. 2015). In this case, Br is very poorly correlated with P (-0.29, p=0.05) which, in turn, is very poorly correlated with other elements usually identified as indicative of organic material (e.g. S and Sr). Conversely, the correlation with Fe is good, and it is likely that P-associated activity had little

to do with accumulation of organic matter and may be linked with, for example, burning or iron-rich peat. Alternatively, Fe might indicate metalworking. It is also possible that concentrations of P were heavily distorted by post-depositional processes. Despite doubts over the precise interpretation of the P results, and because P readings appear naturally distributed, the decision was made not to exclude P from analysis as there is no clear reason to undermine the results from a methodological standpoint. The P distribution is therefore thought to reflect phenomena (not necessarily anthropogenic) that are also a part of site's history.

4.3.3. Class interpretation

Interpretation is based on class chemical composition as well as on their relationship to features across the site, both natural and anthropogenic (Table 4). Insofar as the class spatial distribution had a robust statistical base, the interpretation presented below is to be treated as rather speculative. There are cases where, for separate classes, similar enrichment patterns have been interpreted differently based solely on the class location within site. The background aim behind information presented in this chapter is an attempt to discuss the site's historical development, devoid of any ambition to claim the undisputable.

Class 1 represents the center of the site mean. It shows a moderate depletion in Br. The indistinct character of this class suggests that it might reflect the middle ground or transition between activity zones and undisturbed terrain, or possibly a heavily-used footpath or track (Manzanilla and Barba 1990).

Class 2 shows moderate enrichment in S, Br and moderate depletion in Ca, Zn, and Sr when compared against the site mean. It represents a biogenic group of elements that is likely to be an effect of human impact. Enrichment in S and Br might indicate activities related to sea water or the use of marine equipment (Burton and Price 1990; Chagué-Goff and Fyfe 1996; Leri et al. 2010). Depletion in elements common in plant matter (Ramirez et al. 2002) might be a result of intensive wear of the grass matt and/or again indicate a heavily frequented route (Fernandez et al. 2002).

Class 3 shows strong enrichment in P and Fe as well as moderate enrichment in S and Mn. This class most likely represents the effect of intensive anthropogenic activity. The most significant characteristic of this cluster is elevated P values, presumably arising from the deposition of organic waste (Schleizer and Howes 2000; Holiday and Gartner 2007), or (together with Fe) deposited as a result of the burning of organic matter (Willson et al. 2007), presumably Fe-rich turf. Elevated S and Mn might suggest increased microbial activity and the accumulation of decomposing organic matter (Milek and Roberts 2013; Supplement data table 3).

Class 4 shows strong enrichment in Ti and V, moderate enrichment in Sr, Zn and Ca, strong depletion in Br, and moderate depletion in S and Rb. Both Ti and V are mobilised during the silicate weathering process and are abundant in the deposition zones of watercourses (Shiller and Mao 2000). Sr, Zn and Ca are most likely to be linked with plant organic matter accumulation (Ramirez-Lozano et al. 2002). Br, S and Rb are often considered to be elements representative of the marine domain (Bolter et al. 1964; Riley and Tongudai 1966; Shibagaki et al. 2008; Leri et al. 2010). Their absence from a marine-influenced environment might indicate this signature has been eroded by the stream.

Class 5 shows moderate depletion in S, and moderate enrichment in Ca and Sr. Due to the sample locations, on the coastline, enrichment of these elements is most probably reflective of a marine signature (Broecker 1970; Minoura et al. 1994; de Villiers 1999) imprinted during the prolonged process of shoreline retreat. Depletion in S is, in this case, a rather unexpected result (Casagrande et al. 1977; Chagué-Goff 2010).

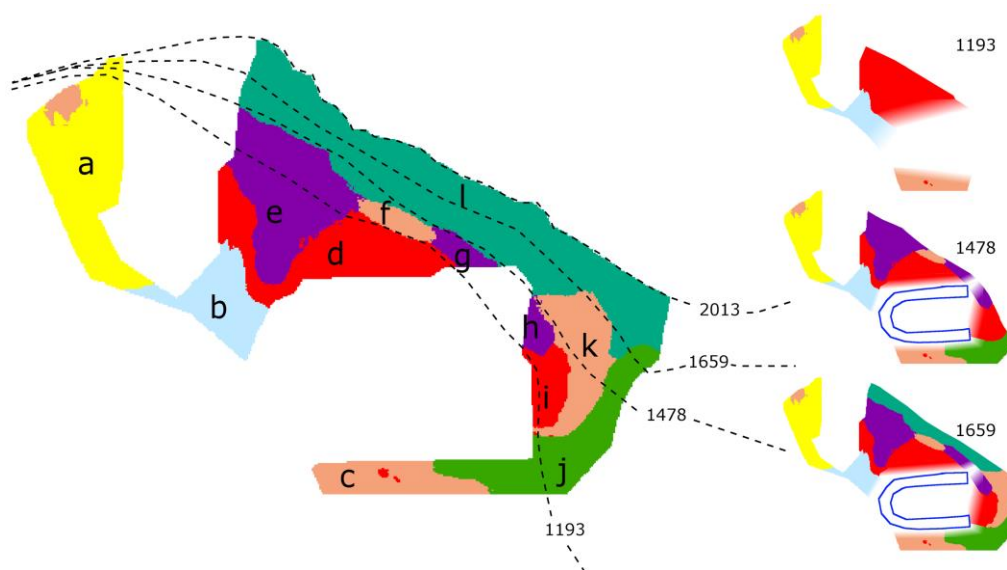
Class 6 shows moderate enrichment in Br, strong depletion in V, Ti, and Fe, and moderate depletion in P, K, Ca, Mn and Zr. Enrichment in Br is most likely due to sea spray (Chen et al. 1997; Shotyk et al. 2003). General depletion in both the lithogenic and organic elements may indicate a sheltered (and unused) area, or anthropogenic alteration possibly linked with the appearance of a depression in the ground. Recent peat cutting might explain the presence of the basin, but its influence on soil geochemistry cannot be established.

Class 7 shows strong enrichment in Br and Rb and moderate enrichment in K and Zr. It also displays strong depletion in Ca and Sr, and moderate depletion in P, Ti, V, Mn and Fe. This class shares some similarities with Class 6 and can be interpreted as an area of low-intensity activity. Its enrichment in lithogenic elements could indicate inorganic sedimentation.

5. Zone interpretation and chronology in relation to RSL change-induced coastline shift

Isochrones marking significant activity episodes identified by Mikolajczyk et al. (2015) have been projected onto the map of identified activity zones for this site (Fig. 7). The matching of isochrones and activity zone edges was surprisingly good except for the area in the vicinity of the dry stream bed. An attempt has been made to present a spatio-chronological model of past coastal activity for this location. In the event of falling RSL, an isochrone-based method can successfully define the timing of onset of human activity. Establishing its cessation is far more problematic due to the possible superimposition of chemical signatures from different processes. Nevertheless, we can speculate about the date for the

348 end of human and create a narrative of the development history for the site.



349

350 Figure 7: left: dashed lines - relative sea level isochrones linked with site activity episodes identified by
351 Mikolajczyk et al. (2015); letters a-l - discrete activity zones. Right- suggested coastal activity development with
352 blue polygon indicating the U-shaped structure. Shading represents missing data. Approximate dates are given
353 in years BC.

354

355 It seems that in late 12th century, 'd' was the first zone active on the coast and it is quite
356 possible that its presence was linked with the V-shaped structure. The zone's location and
357 its chemical character point towards it having been an area of general labour and traffic
358 used for equipment and goods transportation.

359 In the late 15th century, zones 'e', 'f', 'g', 'h', and 'i' became active, probably as a
360 consequence of falling sea level and the emergence of the U-shaped structure. Zone 'e' (and
361 possibly zones of 'g' and 'h') reveal chemical signatures that suggest the deposition of
362 organic waste material and possibly metal working. Zone 'e' probably overlapped with 'd'
363 forming a funnel between two structures that might indicate the presence of a pathway
364 between them. Zones 'g' and 'h' were probably connected though this relationship may be
365 obscured by the collapse of the buildings. Zone 'i' carries a similar chemical fingerprint to 'd'
366 and consequently may be interpreted in the same way (see above).

367 Zone 'f' is determined as having been a liminal area between activity zones and site ridges
368 where the anthropogenic chemical signal was weaker and dispersed.

369 In the following period the emergence of zone 'l' started in the coastal area and it land it
370 was used up until modern times. The unified chemical signature of this zone following the
371 continuously receding coastline since the 15th century suggests that the character of this
372 zone did not change over time. It is most likely to have been unoccupied and subject only to
373 natural effects arising from its proximity to the marine environment.

374 Zone 'k' was probably an extension of 'i' and it seems to have been active until the 17th
375 century. It's chemical characteristics suggests similarity with zone 'f', a peripheral area of
376 activity with a diluted signal.

377 Zone 'j' does not match the sea level isochrones and its extent is most likely linked with the
378 dynamics of the stream. Its emergence might have started together with the earliest activity
379 recorded on site, and its development was most likely interrupted in the 17th century due
380 to the disappearance of the stream.

381 In terms of chronology, location in relation to structures might generally indicate an earlier
382 date for 'a' and 'b' and a later date for 'c'. Despite being close to the shoreline, zone 'a'
383 scores negatively in the marine-influenced principal component (PC1). This may indicate
384 anthropogenic alteration with peat cutting seeming the most reasonable possibility.

385 Zone 'b' has a chemical signature indicating inorganic sedimentation and it correlates with
386 the area that appeared different during sampling as the sediment seemed to be mixed with
387 structural collapse. It is therefore possible that the area's original signature was mixed with
388 the leveled material from the nearby building.

389 Zone 'c' carries a signature similar to the ones interpreted as general working areas. It is
390 likely that it formed a work space linked with the U-shaped structure. Unfortunately this
391 zone lies on the edge of sampled area and the full extent of this unit cannot be traced.

Zone	Class	Class interpretation	elevated elements	depleted elements	chemical signature dating
a	6	sheltered area, peat cutting	Br	V, Ti, Fe P, K, Ca, Mn, Zr	n/a
b	7	mixed, structure collapse	Br, Rb, K, Zr	Ca, Sr, P, Ti, V, Mn, Fe	n/a
c	1	edge of activity zone	n/a	Br	n/a
d	2	general labour, traffic	S, Br	Ca, Zn, Sr	ante 1193
e	3	o.m. deposition, burning, metalworking	P, Fe, S, Mn	n/a	1193
f	1	edge of activity zone	n/a	Br	1193 - (1478)
g	3	o.m. deposition, burning, metalworking	P, Fe, S, Mn	n/a	1193 - (1478)
h	3	o.m. deposition, burning, metalworking	P, Fe, S, Mn	n/a	1193 - (1478)
i	2	general labour, traffic	S, Br	Ca, Zn, Sr	1193 - (1478)

j	4	stream bed, natural	Ti, V, Sr, Zn and Ca	Br, S, Rb	n/a
k	1	edge of activiti zone	n/a	Br	1478 – (1659)
l	5	shoreline, natural	Ca, Sr	S,	1478 - 2013

Table 4. Zone characteristics; class affiliation, functional interpretation, chemical properties and relative sea level-based dating (in brackets are the presumed activity cessation dates).

6. Conclusions

This study has proven successful in applying a multi-elemental dataset to characterise the use of archaeological space on the coast at Vatnsfjörður. The approach can be viewed as an alternative to standard excavation with modest test-pit sampling. The method gives insight into the key factors that shaped local geochemistry and has allowed informed distinctions to be made between anthropogenic pressure and natural processes. We have speculated about the functional use of space across the site and the site's chronology through its relationship to RSL-induced coastal shift. There is plenty of room to further develop the method to incorporate proxies beyond the geochemical suite of elements presented here (e.g. through assessment of biomolecules like proteins, lipids or carbohydrates). This may provide further information about particular activities performed on the site.

7. Acknowledgements

The research was funded through a scholarship awarded by the University of Aberdeen's FAR North programme, and by the Carnegie Trust for the Universities of Scotland. We are very grateful to Fornleifastofnun Islands and the crew of the 2013 field school at Vatnsfjörður for their support with fieldwork, especially Oskar Gísli Sveinbjarnarson, Dawn Elise Mooney and Garðar Guðmundsson. We would also like to express our gratitude to James Parker, Kayleihg Hamilton and OLYMPUS Corporation for providing the 'Olympus-Innov-X Delta Premium XRF' scanner. We are indebted to Edward Schofield for proof-reading and editing the manuscript. We would also like to thank two anonymous reviewers for their insightful comments.

8. References

- Arnalds, O. (2004). Volcanic soils of Iceland. *Catena*, 56, 3-10.
- Arnalds, O., Hallmark, C.T., Wilding, L.P. (1995). Andisols from four different regions of Iceland. *Soil Science Society American Journal*, 59, 161-169.
- Aston, M.A., Martin, M.H., Jackson, A.W. (1998). The use of heavy metal soil analysis for archaeological surveying, *Chemosphere*, 37, 3, 465-477.

- 422 Baxter, M.J. (1995). Standardization and Transformation in Principal Component Analysis, with
423 Applications to Archaeometry. *Applied Statistics-Journal of the Royal Statistical Society Series C*.
424 *Applied Statistics-Journal of the Royal Statistical Society Series C*, 44 ,4, 513-527.
- 425 Blotcky A.J., Falcone, C., Medina, V.A., Rack, E.P., Hobson, D.W. (1979). Determination of trace-level
426 vanadium in marine biological samples by chemical neutron activation analysis. *Analytical Chemistry*,
427 51, 178–182.
- 428 Bolender, D. J. (2006). The Creation of a Propertied Landscape: Land Tenure and Agricultural
429 Investment in Medieval Iceland (unpublished PhD thesis). Northwestern University.
- 430 Bolter, E., Turekian, K. K., Schutz, D. F., (1964).The distribution of rubidium, cesium and barium in
431 the oceans, *Geochimica et Cosmochimica Acta*, 28, 9, 1459-1466.
- 432 Brady, N. C., Weil, R. R. (1999). The nature and properties of soils.
- 433 Burton, J.H.,Price, T.D. (1990). The ratio of barium to strontium as a paleodietary indicator of
434 consumption of marine resources. *Journal of Archaeological Science*, 17, 547-557.
- 435 Casagrande, D. J. , Siefert, K. Berschinski, C., Sutton,N. (1977) Sulfur in peat-forming systems of the
436 Okefenokee Swamp and Florida Everglades: origins of sulfur in coal, *Geochimica et Cosmochimica*
437 *Acta*, 41, 161-167.
- 438 Chagué-Goff, C. (2010). Chemical signatures of palaeotsunamis: A forgotten proxy?, *Marine Geology*,
439 271, 67-71.
- 440 Chagué-Goff, C., Fyfe, W.S. (1996)Geochemical and petrographical characteristics of a domed bog,
441 Nova Scotia: a modern analogue for temperate coal deposits, *Organic Geochemistry*, 24, 141–15.
- 442 Chambers, R. L., Kokic, P., Smith, P., Cruddas, M. (2000). Winsorization for identifying and treating
443 outliers in business surveys. *Proceedings of the 2nd International Conference on Establishment*
444 *Surveys*. Statistics Canada. Ottawa, Canada, 717-726.
- 445 Z. Chen, Z. Chen, W. Zhang (1997)Quaternary stratigraphy and trace-element indices of the Yangtze
446 Delta, Eastern China, with special reference to marine transgressions. *Quaternary Research*, 47, 181–
447 191
- 448 Craig, N., Aldenderfer, M., & Moyes, H. (2006). Multivariate visualization and analysis of
449 photomapped artifact scatters. *Journal of Archaeological Science*, 33, 1617–1627.
- 450 Devereux, B. J., Amable, G. S., & Crow, P. (2008). Visualisation of LiDAR terrain models for
451 archaeological feature detection. *Antiquity*, 82, 470–479.
- 452 Dore, C. D., López Varela, S. L. (2010) Kaleidoscopes, Palimpsests, and Clay: Realities and
453 Complexities in Human Activities and Soil Chemical/Residue Analysis. *Journal of Archaeological*
454 *Method and Theory*, 17, 279-302.
- 455 Entwistle, J.A., McCaffrey, K.J.W., Dodgshon, R.A. (2007) Geostatistical and multi-elemental analysis
456 of soils to interpret land-use history in the Hebrides, Scotland. *Geoarchaeology*, 22, 4, 391-415.

457 ESRI (2015). ArcGIS Desktop: Release 10. Redlands, CA: Environmental Systems Research Institute.

458 Evans, R.T. and Tylecote, R.F., (1967). Some vitrified products of non-metallurgical significance.
459 Bulletin of the Historical Metallurgy Group ,8, 22-23.

460 Fernandez, F.G., Terry, R.E., Inomata, T., Eberl, M. (2002). An ethnoarchaeological study of chemical
461 residues in the floors and soils of Q'eqchi' Maya houses at Las Pozas, Guatemala. *Geoarchaeology*,
462 17, 487–519.

463 Franklin, J. N. (2003). The Role of Vanadium Bromoperoxidase in the Biosynthesis of Halogenated
464 Marine Natural Products. Unpublished PhD Thesis, University of California, Santa Barbara.

465 Guttman, L. (1954). Some necessary conditions for common factor analysis. *Psychometrika*, 19, 149–
466 161.

467 Hayward, C. (2012). High spatial resolution electron probe microanalysis of tephras and melt
468 inclusions without beam-induced chemical modification. *Holocene*, 22, 1, 119-125. Holliday, V.T.,
469 Gartner, W.G. (2007). Methods of soil P analysis in archaeology. *Journal of Archaeological Science*,
470 34, 301-333.

471 Holliday, V. T., Gartner, W. G. (2007). Methods of soil P analysis in archaeology. *Journal of*
472 *Archaeological Science*, 34, 301-333

473 Hotelling, H. (1933). Analysis of a complex of statistical variables into principal components. *Journal*
474 *of Educational Psychology*, 24, 417–441.

475 Ilves, K., Darmark, K. (2011). Some Critical and Methodological Aspects of Shoreline Determination:
476 Examples from the Baltic Sea Region. *Journal of Archaeological Method and Theory*, 18, 147-165.

477 Jagan , A., (2010). Tephra stratigraphy and geochemistry from three Icelandic lake cores: a new
478 method for determining source volcano of tepra layers university of Edinburgh.

479 Kaiser, H.F. (1960). The application of electronic computers to factor analysis. *Educational and*
480 *Psychological Measurement*, 20, 141–151.

481 Kaiser, H.F. (1970). A second generation Little Jiffy. *Psychometrika*, 35 ,401–417.

482 Knudson, K. J., Frink, L., Hoffman, B. W., & Price, T. D. (2004). Chemical characterization of Arctic
483 soils: Activity area analysis in contemporary Yup'ik fish camps using ICP-AES. *Journal of*
484 *Archaeological Science*, 31, 8, 443-456.

485 Küttner, A., Mighall, T. M., De Vleeschouwer, F., Mauquoy, D., Martínez Cortizas, A., Foster, I. D .L.,
486 Krupp, E. (2014). A 3300-year atmospheric metal contamination record from Raeburn Flow raised
487 bog, south west Scotland, *Journal of Archaeological Science*,44, 1-11.

488 Kvamme, K. L. (2006). Integrating multidimensional geophysical data. *Archaeological Prospection*,
489 13, 1, 57–72.

490 Kvamme, K. L. (2007). Integrating multiple geophysical datasets. In Wiseman, J., El-Baz, F.
491 (Eds.), *Remote sensing in archaeology*, New York, Springer, 345–374.

492 Leri, A., Hakala, J., Marcus, M., Lanzirrotti, A., Reddy, C., Myneni, S. (2010). Natural organobromine
493 in marine sediments: New evidence of biogeochemical Br cycling. *Global Biogeochemical Cycles*, 24.

494 Linderholm, J., Lundberg, E. (1994). Chemical Characterization of Various Archaeological Soil Samples
495 using Main and Trace Elements determined by Inductively Coupled Plasma Atomic Emission
496 Spectrometry. *Journal of Archaeological Science*, 21, 3, 303-314.

497 Lloyd, J.M., Dickens, W. (2011). Relative sea-level change and coastal evolution from Sveinhúsavatn,
498 Vatnsfjörður, NW Iceland. Unpublished report for Fornleifastofnun Islands.

499 Lutz, H. J. (1951) Concentration of Certain Chemical Elements in the Soils of Alaskan Archaeological
500 Sites. *American Journal of Science*. 249, 12, 925-928.

501 Manzanilla, L., Barba, L. (1990). The Study of Activities in Classic Households: Two Case Studies from
502 Coba and Teotihuacan. *Ancient Mesoamerica*, 1, pp 41-49

503 Mayer, L. M., Macko, S. A., Mook, W. H., Murray, S. (1981). The distribution of bromine in coastal
504 sediments and its use as a source indicator for organic matter. *Organic Geochemistry*, 3, 37-42.

505 Middleton, W. D., Price, T. D. (1996) (with) Chemical Analysis of Modern and Archaeological House
506 Floors by Inductively Coupled Plasma- Atomic Emission Spectroscopy. *Journal of Archaeological
507 Science* 23 (5): 673-687.

508 Middleton W. D., Barba L., Pecci A., Burton J.H, Ortiz A., Salvini L., Rodriguez Suárez R. (2010). The
509 Study of Archaeological Floors: Methodological Proposal for the Analysis of Anthropogenic Residues
510 by Spot Tests, ICP-OES, and GC-MS. *Journal of Archaeological Method and Theory*, 17, 183-208.

511 Mikołajczyk, Ł. (2013). Chemical properties of possible floor deposit [12026] from structure 5 (Area
512 45, VSF12). In: Isaksen, O. (Ed.), *Vatnsfjörður 2012: Framvinduskýrslur/Interim Report*.
513 Fornleifastofnun Islands, Reykjavík, pp. 56E60. Available from:
514 [http://www.instarch.is/pdf/uppgraftarskyrslur/FS514-
515 030912_Vatnsfj%C3%B6r%C3%B0ur%202012.pdf](http://www.instarch.is/pdf/uppgraftarskyrslur/FS514-030912_Vatnsfj%C3%B6r%C3%B0ur%202012.pdf) (12.04.16.).

516 Mikołajczyk, Ł., Gardeła, L. (2010). GPS survey in the coastal area of Vatnsfjörður. In: Milek, K. (Ed.),
517 *Vatnsfjörður 2009: Framvinduskýrslur/Interim Report*. Fornleifastofnun Islands, Reykjavík, pp. 41-
518 50. Available from: [http://www.instarch.is/pdf/uppgraftarskyrslur/FS449-
519 03099_Vatnsfj%C3%B6r%C3%B0ur%202009.pdf](http://www.instarch.is/pdf/uppgraftarskyrslur/FS449-03099_Vatnsfj%C3%B6r%C3%B0ur%202009.pdf) (19.04.16.).

520 Mikołajczyk, Ł., Ilves, K., May, J., Sveinbjarnarson, O., Milek, K. (2015). Use of phosphorus mapping in
521 assessing coastal activity zones of an Icelandic multi-period site of Vatnsfjörður, *Journal of
522 Archaeological Science*, 59, 1-9.

523 Milek, K. (2011). Samantekt/Overview. In: Milek, K. (Ed.), *Vatnsfjörður 2010:
524 Framvinduskýrslur/Interim Report*. Fornleifastofnun Islands, Reykjavík, 15-24. Available from:
525 [http://www.instarch.is/pdf/uppgraftarskyrslur/FS461-
526 030910%20Vatnsfj%C3%B6r%C3%B0ur%202010%20Interim%20Reports.pdf](http://www.instarch.is/pdf/uppgraftarskyrslur/FS461-030910%20Vatnsfj%C3%B6r%C3%B0ur%202010%20Interim%20Reports.pdf) (10.05.16.).

527 Milek, K. B., Roberts, H. M. (2013). Integrated geoarchaeological methods for the determination of
528 site activity areas: A study of a Viking Age house in Reykjavik, Iceland. *Journal of Archaeological*
529 *Science*, 40, 4, 1845-1865.

530 Minoura, K., Nakaya, S., Uchida, M. (1994). Tsunami deposits in a lacustrine sequence of the Sanriku
531 coast, northeast Japan, *Sedimentary Geology*, 89, 25–31.

532

533 Misarti, N., Finney B., and Maschner H. (2011). Reconstructing site organization in the eastern
534 Aleutian Islands, AK using multi-element chemical analysis of soils. *Journal of Archaeological Science*
535 38, 7, 1441-1455.

536 Mooney, D.E. (2011). Evaluation trenches excavated at vatnsfjörður. In: Milek, K. (Ed.),
537 *Vatnsfjörður 2010: Framvinduskýrslur/Interim Report*. Fornleifastofnun Islands, Reykjavík, pp.
538 69e75. [http://www.instarch.is/pdf/uppgraftarskyrslur/FS461-030910%20Vatnsf](http://www.instarch.is/pdf/uppgraftarskyrslur/FS461-030910%20Vatnsf%20%C3%B6r%C3%B0ur%202010%20Interim%20Reports.pdf)
539 [%20%C3%B6r%C3%B0ur%202010%20Interim%20Reports.pdf](http://www.instarch.is/pdf/uppgraftarskyrslur/FS461-030910%20Vatnsf%20%C3%B6r%C3%B0ur%202010%20Interim%20Reports.pdf) (06.05.16.).

540 Mooney, D.E., Sveinbjarnarson, O.G., Mikołajczyk, Ł. (2012). Evaluation trenches and Excavations of
541 the coastal structures at vatnsfjörður. In: Isaksen, O. (Ed.), *Vatnsfjörður 2011:*
542 *Framvinduskýrslur/Interim Report*. Fornleifastofnun Islands, Reykjavík, pp. 47e64. Available from:
543 [http://www.instarch.is/pdf/uppgraftarskyrslur/FS492-](http://www.instarch.is/pdf/uppgraftarskyrslur/FS492-030911_Vatnsfj%C3%B6r%C3%B0ur%202011.pdf)
544 [030911_Vatnsfj%C3%B6r%C3%B0ur%202011.pdf](http://www.instarch.is/pdf/uppgraftarskyrslur/FS492-030911_Vatnsfj%C3%B6r%C3%B0ur%202011.pdf) (08.05.16.).

545 Mooney, D.E. (2013). Excavations of the Coastal structures at vatnsfjörður: areas 45 & 46. In:
546 Isaksen, O. (Ed.), *Vatnsfjörður 2012: Framvinduskýrslur/Interim Report*. Fornleifastofnun Islands,
547 Reykjavík, pp. 40e55. Available from: [http://www.instarch.is/pdf/uppgraftarskyrslur/FS514-](http://www.instarch.is/pdf/uppgraftarskyrslur/FS514-030912_Vatnsfj%C3%B6r%C3%B0ur%202012.pdf)
548 [030912_Vatnsfj%C3%B6r%C3%B0ur%202012.pdf](http://www.instarch.is/pdf/uppgraftarskyrslur/FS514-030912_Vatnsfj%C3%B6r%C3%B0ur%202012.pdf) (08.05.16.).

549 Norðdahl, H., Petursson, H.G. (2005). Relative sea-level changes in Iceland; new aspects of the
550 Weichselian Deglaciation of Iceland. In: Caseldine, C., Russel, A., Hardardottir, J., Knudsen, O. (Eds.),
551 *Iceland e Modern Processes and Past Environments*, 25-78.

552 Olsen, D. J. R., Endelman, J. B., Jacobson, A. R., Reeve, J. R. (2015). Compost Carryover: Nitrogen
553 Phosphorous and FT-IR Analysis of Soil Organic Matter . *Plants, Soils, and Climate Faculty*
554 *Publications*. Paper 733.

555 Oonk S., Slomp, C. P., Huisman, J. D. (2009). Geochemistry as an aid in archaeological prospection
556 and site interpretation: current issues and research directions. *Archaeological Prospection*, 16, 35–
557 51.

558 Pearson, K., (1901) On lines and planes of closest fit to systems of points in space. *Philosophical*
559 *Magazine*, Series 6, 2, 559–572.

560 R Core Team. (2014). R: A language and environment for statistical computing. R Foundation for
561 Statistical Computing, Vienna, Austria.

562 Ramirez L., Roque, G., Humberto, G. R., Guillermo, G. D. (2002). Chemical composition and rumen
563 digestion of forage from kleingrass (*panicum coloratum*). *INCI* , 27, 12, 705-709.

564 Richards, J. A., & Jia, X. (1999). Remote sensing digital image analysis: An introduction. New York:
565 Springer.

566 Schiller, A.M., Mao, L. (2000). Dissolved V in rivers: effects of silicate weathering. *Chemical Geology*,
567 165, 13–22.

568 Schlezinger, D.R. and B.L. Howes. (2000). Organic phosphorus and elemental ratios as indicators of
569 prehistoric human occupation. *Journal of Archaeological Science* , 27, 479-492.

570 Schofield, J. E., Edwards, K. J., Mighall, T. M., Martínez Cortizas, A., Rodríguez-Racedo, J., Cook, G.
571 (2010) An integrated geochemical and palynological study of human impacts, soil erosion and
572 storminess from southern Greenland since c. AD 1000. *Palaeogeography, Palaeoclimatology*,
573 *Palaeoecology*, 295, 19–30.

574 Shibagaki, N., Pootakham, W., Grossman, A. R. (2008). The responses of algae to their sulfur
575 environment. In *Advances in Photosynthesis and Respiration*. Hell, R. Dahl, C., Knaff, D., Leustek, T.
576 (Eds). *Invited Review*, 231-267.

577 Shotyk, W. (1988). Review of the inorganic geochemistry of peats and peatland waters. *Earth-*
578 *Science Reviews*, 25, 95–176.

579 Simpson, I.A., Adderley, W.P., Guðmundsson, G., Hallsdottir, M., Sigurgeirsson, M.A., Snæsdottir, M.
580 (2002). Soil limitations to agrarian land production in premodern Iceland. *Human Ecology*, 30, 4, 423-
581 443.

582 de Villiers S. (1999) Seawater strontium and Sr/Ca variability in the Atlantic and Pacific oceans. *Earth*
583 *and Planetary Science Letters* 171, 623-634.

584 Turekian K. K. (1964). The marine geochemistry of strontium. *Geochimica et Cosmochimica Acta*, 28,
585 1479–1496.

586 Wilson, C.A., Davidson, D.A., Cresser, M.S. (2007). Evaluating the use of multi-element soil analysis in
587 archaeology: a study of a post-medieval croft (Olligarth) in Shetland. *Atti della Società Toscana di*
588 *Scienze Naturali* 112, 69–78.

589 Wilson, C. A., Davidson, D. A., Cresser, M.S. (2009). An evaluation of the site specificity of soil
590 elemental signatures for identifying and interpreting former functional areas, *Journal of*
591 *Archaeological Science*, 36, 10, 2327-2334.

592 Ziegler, M., Jilbert, T., de Lange, G. J., Lourens, L. J., Reichert, G. J. (2008). Bromine counts from XRF
593 scanning as an estimate of the marine organic carbon content of sediment cores. *Geochemistry*,
594 *Geophysics, Geosystems*, 9, 1525-2027.

595